In: Spectroscopic Techniques for Security, Forensic ... ISBN: 978-1-63117-404-9
Editors: Y. Dwivedi, S. B. Rai and J. P. Singh

Chapter 8

VANADIUM OXIDES FOR ENERGY AND SECURITY APPLICATIONS

Chiranjivi Lamsal and N. M. Ravindra*

New Jersey Institute of Technology, Newark, New Jersey, US

Vanadium oxides have been the active area of research for decades and new possibilities are being revealed day by day due to their well established, yet controversially explained, phenomenon of Insulator Metal phase Transition (IMT). In this study, we have summarized potential solutions to the challenges in the fields of energy, environmental protection, defense and security that are being faced by the world. These challenges include security of energy supply, increasing demand of expensive energy, energy shortage and exploration of new source of energy and minerals, resolving fluctuating energy cost, CO_2 emission associated with energy consumption, climate change, and potential threat regarding the security of people and the country. The role of vanadium oxides in smart materials, their working principle and mechanism, methods for enhancing their performances, parameters controlling their efficiency, spectral range for optimum performance and source of operations have been described. The complicacy of thermal detectors and the use of vanadium oxides as sensing elements in such detectors have been explained and practical examples are presented. The performance parameters of a bolometer detector are illustrated from the data available in the literature. Use of vanadium oxides as a sensing element in stable, high TCR (Temperature Coefficient of Resistance) bolometer operating at room temperature in the flat spectral range without any cooling mechanism has been described and the importance of passivation characteristics, good IR (Infra Red) absorption characteristics and fabrication compatibility of vanadium oxides to modern technology has been highlighted. Recent progress in the dynamic tuning of metamaterials achieved by blending the properties of the VO_2 film during the IMT is described.

* Email: nmravindra@gmail.com.

1.1. INTRODUCTION

The ground state electronic configuration of vanadium is $[Ar]3d^3 4s^2$. Being a d-transition metal, vanadium has different oxidation states capable of existing in both single as well as mixed valence state on forming oxides. The vanadium oxides such as VO, V_2O_3, VO_2 and V_2O_5 exist in a single oxidation state whereas many others, for instance: V_3O_5, V_4O_7, V_6O_{11}, V_6O_{13}, V_7O_{13}, V_8O_{15} etc., remain in mixed (two) valence state. However, these oxides can be categorized under the so-called Magnéli (V_nO_{2n-1}) and Wadsley ($V_{2n}O_{5n-2}$) homologous series. Di-, Sesqui- and pentoxides of vanadium (VO_2, V_2O_3 and V_2O_5) are most widely studied oxides of vanadium for technological applications. Vanadium ions in VO_2 and V_2O_3 have $V^{4+}(d^1)$ and $V^{3+}(d^2)$ electronic structures whereas V_2O_5 has V^{5+} ion with no 3d electrons. In these transition metal oxides, d electrons are spatially confined in partially filled orbitals and are considered to be strongly interacting or "correlated" because of Coulombic repulsion between two d electrons of opposite spin on the same ion. In other words, the two conduction electrons with antiparallel spin at the same bonding site repel each other with strong Coulomb force so as to keep them mutually separated and hence spatially localized in individual atomic orbitals rather than behaving as delocalized Bloch functions. Correlated electrons are responsible for the extreme sensitivity of materials for small change in external stimuli such as pressure, temperature or doping [1].

Several vanadium oxides undergo insulator-metal transitions (IMT) at a particular temperature, T_c. The IMT, occurring in these materials, varies over a wide range of temperatures and depends on the O/V ratio, i.e., the transition temperature increases with oxidation states of the vanadium atom [2]. Among them, VO_2 is one of the widely studied materials which undergoes IMT at 340K [3], while V_2O_3 and V_2O_5 exhibit transitions at 160K [4] and 530K [5] respectively. These first order phase transitions are reversible [6] and are accompanied by drastic change in crystallographic, optical and electrical properties. During structural transition, atoms undergo displacement with redistribution of electronic charge in the crystal lattice and hence the nature of interaction changes [7]. Below T_c, the V-O system shows insulating behavior wherein VO_2 and V_2O_3 have monoclinic structure [8, 9] and V_2O_5 has orthorhombic structure [10]. At temperatures greater than T_c, they behave like metal but with crystal structures that are different from their low temperature counterparts [8, 11]. Similarly, the phase transition leads to change in electrical conductivity up to 10 orders of magnitude [12], while optical properties show discontinuity.

The vanadium oxides are chromogenic materials and can change their optical properties due to some external stimuli in the form of photon radiation (photochromic), change in temperature (thermochromic) and voltage pulse (electrochromic); the change becomes discontinuous during IMT. Such properties can be exploited to make coatings for energy-efficient "smart windows" [13], and electrical and optical switching devices [14]. Thin films of VO_2 and V_2O_3 have been found to show good thermochromism in the infrared region [15, 16]. While maintaining the transparency to visible light, a smart window modulates infrared irradiation from a low-temperature transparent state to a high-temperature opaque state [17]. The two oxides, VO_2 and V_2O_5, can change their optical properties in a persistent and reversible way in response to a voltage [18]. V_2O_5 exhibits exceptional electrochromic behavior because it has both anodic and cathodic electrochromism, different from VO_2 which only has anodic electrochromism. These electrochromic materials have four main

applications: information displays, variable-reflectance mirrors, smart windows and variable-emittance surfaces.

The V-O systems are widely applicable in technology such as memory devices and temperature sensors [19]. The memory aspect of the material is evidenced from the pronounced hysteresis present in phase transition [20]. Normally the range of operation of a device lies outside the hysteresis region. However, some bolometric devices are operational within the hysteretic transition [21]. Bolometers are thermal infrared (IR) detectors and can be used in infrared imaging applications such as thermal camera, night vision camera, surveillance, mine detection, early fire detection, medical imaging, and detection of gas leakage. A bolometer requires a material with high temperature coefficient of resistance (TCR) and a small 1/f noise constant [22]. Pure, stoichiometric single-crystals of VO_2 and V_2O_5 have high TCR but are difficult to grow. Furthermore, the latent heat involved in IMT is highly unfavorable for the bolometric performance [23]. Since T_c of V_2O_3 is far below room temperature, the resistance and hence the level of noise is low which makes V_2O_3 a good candidate for the fabrication of efficient microbolometers. However, Cole et al. [24] have shown that the thin films of all the three oxides, combined together, can produce a desired material with high TCR and optimum resistance for bolometer fabrication.

Clearly, phase transition in VO_2 is of high technological interest. IMT occurs near to room temperature and T_c can be tuned optically, thermally, electrically [25] and with doping [12]. The phase transition in VO_2 has been used to achieve frequency-tunable metamaterials in the near-infrared range [26, 27]. Recently, Kyoung et al. [28] have extended the study to terahertz range proposing an active terahertz metamaterial, a gold nano-slot antenna on a VO_2 thin film, which transforms itself from transparent to complete extinct at resonance when the VO_2 film undergoes thermo or photoinduced phase transition. Cavalleri et al. [8] showed that the phase transition can be photoinduced within hundreds of femtoseconds which can be an underlying principle for an ultrafast switch.

1.2. SMART MATERIALS

Highly sensitive materials which can change their properties reversibly and persistently as a response to external stimuli such as pressure, temperature, light, electric fields, magnetic fields or chemical stimulus are called smart materials. A number of smart materials have been discovered such as [29] color- and optically changing smart materials (able to change color and or optical properties), adhesion-changing smart materials (able to change the attraction forces of adsorption or absorption of an atom or molecule), light-emitting smart materials (able to emit light by a phenomenon called luminescence), electricity-generating smart materials (able to generate an electric current), energy exchanging smart materials (able to store both sensible and latent energy and exhibit some reversibility), material-exchanging smart materials (able to bind and release matter), and even shape-changing smart materials (able to change shape and/or dimensions). Smart materials are being utilized to meet the increasing demand for expensive energy sources and raw materials, enhanced applications in automation, compact materials and products reacting to sensors and actuators. Since vanadium oxides are chromogenic, our focus will be on the chromogenic smart materials. Chromogenic smart materials are being widely used for architectural glazing, transportation

and certain electronic displays. The concept of architectural glazings and the use of smart materials in vehicles (rear view mirrors, sun-roofs, visors, etc), aircrafts, spacecrafts and ships have been very attractive.

Chromogenic technologies are based on various mechanisms such as [30]: electrochromism, electrophoresis, liquid crystal display, thermotropics, photochromism, and thermochromism. However, the common feature of these technologies is the ability of the material to switch optical transmittance and reflectance. For quantifying these optical properties, average transmittance and reflectance quantities are defined based on their transmittance, $T(\lambda)$, and reflectance spectra, $R(\lambda)$. Some of such quantities are solar and visible (or luminous) transmittance and reflectance defined as [31]:

$$T_{sol} = \frac{\int_0^\infty T(\lambda)\varphi_{sol}(\lambda)d\lambda}{\int_0^\infty \varphi_{sol}(\lambda)d\lambda}, \quad R_{sol} = \frac{\int_0^\infty R(\lambda)\varphi_{sol}(\lambda)d\lambda}{\int_0^\infty \varphi_{sol}(\lambda)d\lambda} \tag{1.1}$$

$$T_{vis} = \frac{\int_{370}^{770} T(\lambda)\varphi_{vis}(\lambda)d\lambda}{\int_{370}^{770} \varphi_{vis}(\lambda)d\lambda}, \quad R_{vis} = \frac{\int_{370}^{770} R(\lambda)\varphi_{vis}(\lambda)d\lambda}{\int_{370}^{770} \varphi_{vis}(\lambda)d\lambda} \tag{1.2}$$

where, $\varphi_{vis}(\lambda)$ refers to the visible spectral range of 0.37-0.77 μm and $\varphi_{sol}(\lambda)$ refers to 0.25 -3 μm interval of solar radiation. A smart window, for example, capable of transmitting the visible radiation should have high T_{vis} while for the purpose of reflecting heat, it should have low T_{sol} and high R_{sol}.

Smart windows are physical counter parts of biological cell walls, which adjust energy flow in accord with the thermal and optical need of the house such as light, view or privacy and hence can be considered as a salient feature of a home automation system that offers interactive security. The term, smart window, applies to a glass that can manually or automatically change the intensity of light passing through it. The use of switchable glazings in buildings results in reduction in energy used for heating, cooling and lighting. The world is facing two major challenges: security of its energy supply and climate change. Obviously, the most secure energy is saved energy and reducing the energy consumption will help to reduce the CO_2 emission caused by energy generation.

(a) Smart glass “off” (b) Smart glass “on”

Figure 1. Smart window in “OFF” and “ON” state [32].

1.2.1. Electrochromism

Electrochromic phenomenon was first invented in tungsten oxide thin films (WO_3) in 1969 [33] and, since then, researchers have focused on a wide range of materials and device structures. A number of alternate optical switching systems have been developed and in the mid-1980s, Granqvist coined a phrase "smart window" to describe electrochromic glazings [31]. Electrochromic material can regulate the transmittance (T), reflectance (R), absorption (A) and emittance (E) upon the application of a voltage between widely separated extrema [34]. In other words, an electrochromic material changes color persistently and reversibly by an electrochemical reaction between a transparent ("bleached") state and a colored state as shown in Figure 1 or between two colored states. This optical change occurs as a result of a small electric current at low dc potentials, well within a few volts [35].

An electrochromic device mainly consists of a configuration of three layers, each with less than one micrometer thick, positioned on a substrate or between two substrates: an ion storage film, an ion conductor (electrolyte) and an electrochromic film sandwiched between electrically conducting films (the electrodes) as shown in Figure 2. On applying an electric field, the ions which are normally small with high mobility such as H^+ or Li^+, move from the ion storage layer into the electrochromic layer via the ion conductor. The external electric circuit provides charge-balancing (an electronic charge equal to ionic charge) counterflow of electrons which creates a variation in the electron density in the electrochromic materials. These electrons also remain in the electrochromic film for the time the ions reside there altering, thereby, the optical properties. If the electrolyte is a pure ion conductor with negligible electronic conductivity, the device acquires the state of open state memory and electric field is not required unless it is desired to change the optical property. The electron injection can alter the transparency depending on the nature of the electrochromic oxide used. Ideally, this process is reversible so that the material returns to a transparent state with the extraction of the ions and electrons. The main requirements of the electrochromic film used in such devices are as follows:

a Coloration efficiency: optical modulation should be commensurate with the finite change in the electron density.
b Ion intercalation and deintercalation: The electrochromic film darkens up as the ions (H^+ or Li^+, etc.) move uniformly into and out of the electrochromic film. Hence it is required that insertion and extraction of ions through the film be easy.

If ion intercalation (insertion) leads to the darkening of the film, the coloration is said to be cathodic, whereas, deintercalation (extraction) led coloration is known as anodic coloration [18]. In other words, charge injection in cathodic electrochromic process leads to a decrease in transmittance while in anodic electrochromism, the injection leads to an increase in transmittance. The ion storage film, in this device, can be chosen with or without electrochromic property. The electrochromic storage film - the counter electrode- in variable light transmission electrochromic devices, such as smart windows, should be chosen in such a way that it works in a mode that is complimentary to the primary electrochromic material. In other words, the counter electrode should darken upon ion intercalation if the primary electrochromic film –the working electrode- darkens upon ion deintercalation and vice versa.

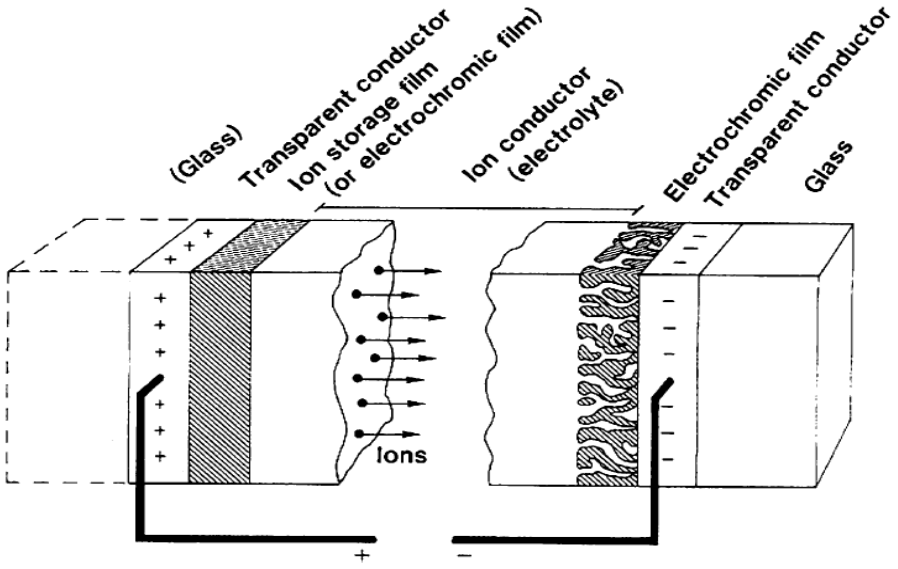

Figure 2. Schematic of an electrochromic device [34] showing the motion of positive ions.

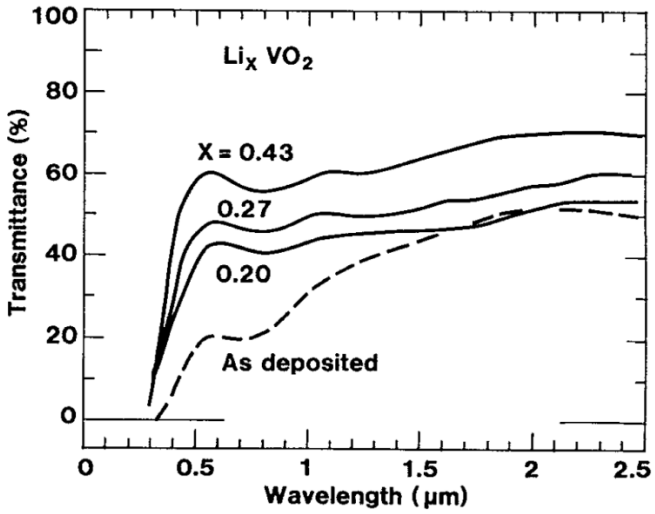

Figure 3. Transmittance spectra of 170 nm thick VO_2 film before and after lithiation [36].

VO_2 and V_2O_5 are electrochromic materials - VO_2 shows anodic coloration whereas V_2O_5 shows exceptional behavior of both types of coloration phenomenon within different wavelength ranges [18]. Other inorganic electrochromic systems are: WO_3, NiO, TiO_2, IrO_2, Nb_2O_5, SnO_2 and Pr_2O_3 among which WO_3 has the most electrochromic efficiency observed so far. In an attempt to see the improved performance of vanadium oxide as an electrochromic film, Khan et al. [36] studied transmittance spectra of Li-intercalated film of VO_2 (Li_xVO_2) at room temperature and found that the intercalation of lithium leads to a large increase in transmittance. Interestingly, such effect is observed over all spectral range with visible region showing the most pronounced change as shown in Figure 3. Achieving high transmittance modulation seems possible by combining anodically coloring Li_xVO_2 film with a cathodically

coloring Li_yWO_3 film [36]. In similar studies [37, 38] of Li-intercalated film of V_2O_5 ($Li_xV_2O_5$), thermochromism is found to be weaker and of more complex nature. However, it has been realized that V_2O_5 films have electrochromic properties that are appropriate for counter electrode material for electrochromic devices. In their study, Cogan et al. [37] concluded that V_2O_5 shows a yellow to colorless modulation for a typical choice of film thickness (120nm) with Li^+ insertion level of 10-15mC/cm^2. Hence V_2O_5 film is a good potential counter electrode to WO_3 in electrochromic devices. V_2O_5 is particularly interesting not only because it has an excellent (charge) capacity to incorporate (Li^+) ions [39] but also due to relative ease of production by using simple, inexpensive and non-toxic sol-gel deposition technique. In a WO_3-V_2O_5 electrochromic device, the overall electrochemical reaction occurs as [37]:

$$a - Li_xWO_3 + V_2O_5 \Leftrightarrow a - WO_3 + Li_yV_2O_5$$

The absorption in the layers, Li_xWO_3 and V_2O_5, occurs in the red and blue spectral region, respectively, while thin film of $a - WO_3$ and $Li_yV_2O_5$ are transparent and colorless. Hence the WO_3 and V_2O_5 work synchronously as a complementary pair giving coloring and bleaching action in the electrochromic device.

Electrochromism can be explained theoretically in terms of a band-structure model. For a 0.1 μm thick film of $Li_xV_2O_5$ made with the substrate temperature of 50^{o}C and 300^{o}C, Talledo et al. [40] found the structure of the films to be nanocrystalline and polycrystalline respectively. On changing the doping level from x=0 to 1.5 in the nanocrystalline state, the band gap increased proportionally with x from 2.25 to 3.1 eV. For polycrystalline film, there was a shift in band gap from 2.38 eV at x=0 to 2.75 eV at x=2.2. However, the shift was not proportional to x, unlike in the nanocrystalline structure. The shift was predominant at x=1.0. It was observed that the absorption at $\lambda > 0.5\ \mu m$ increased with increase in the doping level from x=0 to 1.0 and then decreased for x=1.0 to > 2.0. This observation can be understood, at least qualitatively, with band structure effect and polaron absorption.

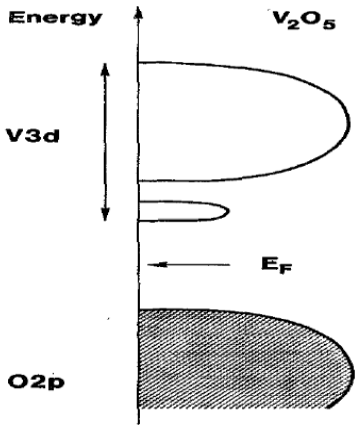

Figure 4. Schematic sketch of density of states for V_2O_5 [40].

The density of states for V_2O_5 can be represented schematically as shown in Figure 4 where O2p states are filled and V3d states are empty. As can be seen in Figure 4, the most bonding part of the d band is split-off from the d band spectrum [40, 41] and the optical band gap is the difference in energy between the top of the O2p band and the bottom of the split-off part of the V3d band, with Fermi level (E_F) lying in the gap. However, the insertion of ions and electrons shifts E_F to the split off band. With the increased ion intercalation, the split-off component gets filled up. Parity selection rule avoids the transition between the two parts of the d-band and hence the optical band gap is redefined as the difference between the top of the O2p band and the bottom of the main part of the V3d band. The observed [18] decrease in absorptance (increase in transmittance) of the blue light can be related to this band gap widening, giving ultimate explanation of the electrochromism based on band structure. Furthermore, V_2O_5 is known to exhibit cathodic coloration in the near-infrared (near IR) region of the spectrum, where it shows increase in absorptance (decrease in transmittance). This increased absorption is thought to arise from oxygen vacancies in the V_2O_5 lattice. Empty 3d orbitals of vanadium atoms, adjacent to such vacancies, localize $3d^1$ electron states within the band gap producing V^{4+} pairs. These V^{4+} states are responsible for creating small polarons resulting in increased near IR absorption.

1.2.2. Thermochromism

Thermochromism in vanadium oxide materials represents another possibility for smart coating in energy efficient buildings. Thin film of VO_2 is one of the most durable thermochromic materials undergoing IMT at 65 ^oC [42], which is close to its bulk value [3]. However, several techniques such as [43] (a) doping with suitable materials such as tungsten (W), Molybdenum (Mo), Niobium (Nb) and Rhenium (Re) (b) fluorination: replacement of some oxygen atoms by fluorine (c) mechanical stress induced by an over layer, can lower the transition temperature making it quite suitable as a window coating. Figure 5a shows the normal transmittance spectra for VO_2 film at temperatures below and above T_c, measured in the wavelength range of 0.3 to 2.5 μm [44]. For higher wavelengths (the near infrared region, greater than ~0.7 μm), the transmittance is modulated considerably as a function of temperature as compared to the low wavelength region, which is central to an efficient, energy controlling smart window. It means, for wavelengths near infrared, temperature dependent modulation of transmission spectra is observed while maintaining transparency to visible light. At the same time, the near infrared reflectance increases appreciably above T_c in line with the decrease in corresponding transmittance. For use of materials in glazing technology, transmission of light and also the reflectivity (in most applications) are very important. Ideally, a glazing material transmits solar radiation from exterior to interior when the "window" conducts heat out of the building during daytime in the winter and reflects solar radiation when it conducts heat into the building during daytime in the summer.

The transition temperature T_c of W-doped thin film of VO_2 drops almost linearly when the level of doping increases [42]. Sobhan et al. [42] showed that W-doped film, with the composition of $W_{0.032}V_{0.968}O_2$, undergoes IMT at ~32 ^oC and the normal transmittance for this structure varies as shown in Figure 5b. While doping decreases T_c to a comfort temperature, the thermochromic modulation of infrared transmittance, on the other hand, becomes small for the doped sample making it less useful for the energy control in smart windows. Later, in

an attempt to improve the material performance, Granqvist [43] studied the transmittance spectra by replacing some of the oxygen with fluorine at various temperatures as shown in Figure 6. For a 0.13 μm thick VO_xF_y coating, the T_c was found to decrease to 52 ^oC and the near infrared transmission was found to be strongly temperature dependent. In this case, visible transmittance was found to be 28%, irrespective of the temperature and the solar transmittance was noticed to be ranging from 35% at room temperature to 28% at 70^oC. The decrease in T_c and increase in transmittance in the visible spectrum show that VO_2 can be a very good candidate for thermochromic smart window application.

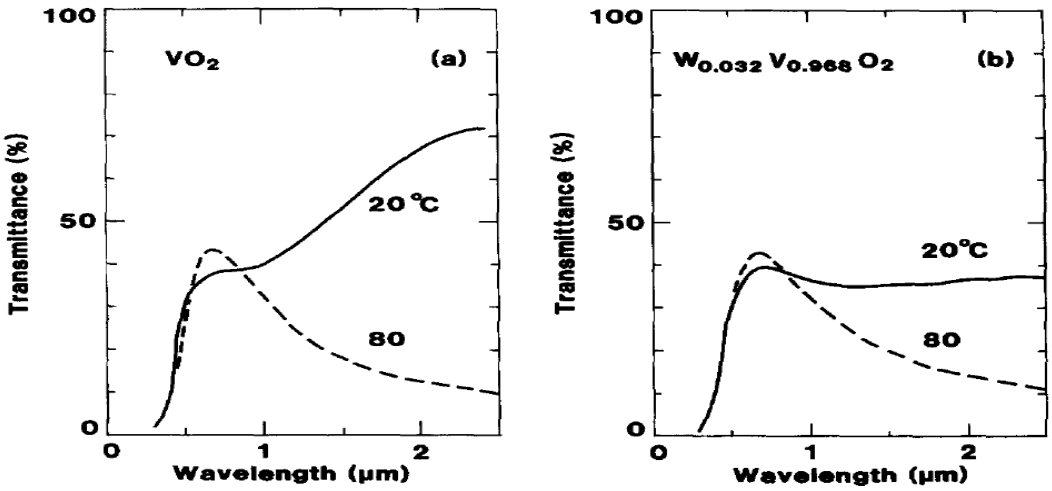

Figure 5. Transmittance spectra for (a) VO_2 and (b) W-doped VO_2 films at temperatures below and above IMT [42].

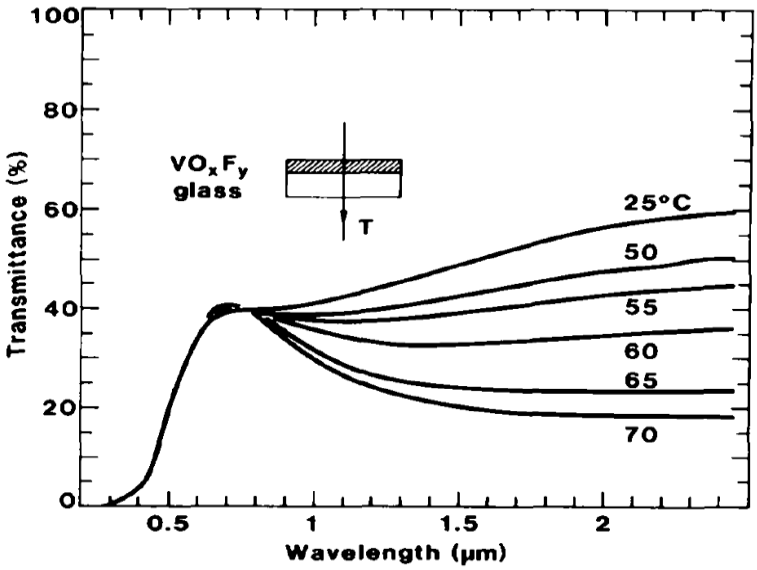

Figure 6. Normal transmittance spectra for vanadium oxyfluoride film at various temperatures [43].

1.3. THERMAL DETECTORS

Any object, from human body to stars, having temperature above absolute zero emits electromagnetic waves depending on its emissivity and its absolute temperature (Stefan-Boltzmann law). In order to detect radiation, we use a photodetector, a device which converts the absorbed photons into a measurable form. There are mainly two types of detectors: photon detectors and thermal detectors. A photon detector is an optoelectronic device which gives rise to an electrical output signal when energy distribution of electrons changes as a result of the interaction of radiation with either free or bound charge carriers in a material. Interaction can be either internal or external. In internal interaction, photons either interact with charge carriers (bound or free) or produce a localized excitation of an electron to higher energy state [45]. However, in external interaction, electrons are emitted as a result of Einstein's photoelectric effect. On the other hand, thermal detectors absorb the photon energy and convert it into heat which, in turn, affects physical or electrical parameters such as electrical conductivity, thermoelectric voltage, and pyroelectric voltage. Hence thermal detectors do not depend on the nature of photon or spectral content of the radiation but depend on radiant power. Since heating and cooling are slower processes compared to interaction between photons and electrons, thermal response is relatively slower than spectral response. Typically, thermal effects occur in millisecond time scale while the effects due to photons are observed on micro or nano second time scale.

Figure 7 shows a schematic representation of a thermal detector. The sensing element, having thermal capacity C, is mounted on a substrate and thermally linked to a heat sink, at a constant temperature T_0, such that the average thermal conductance is G.

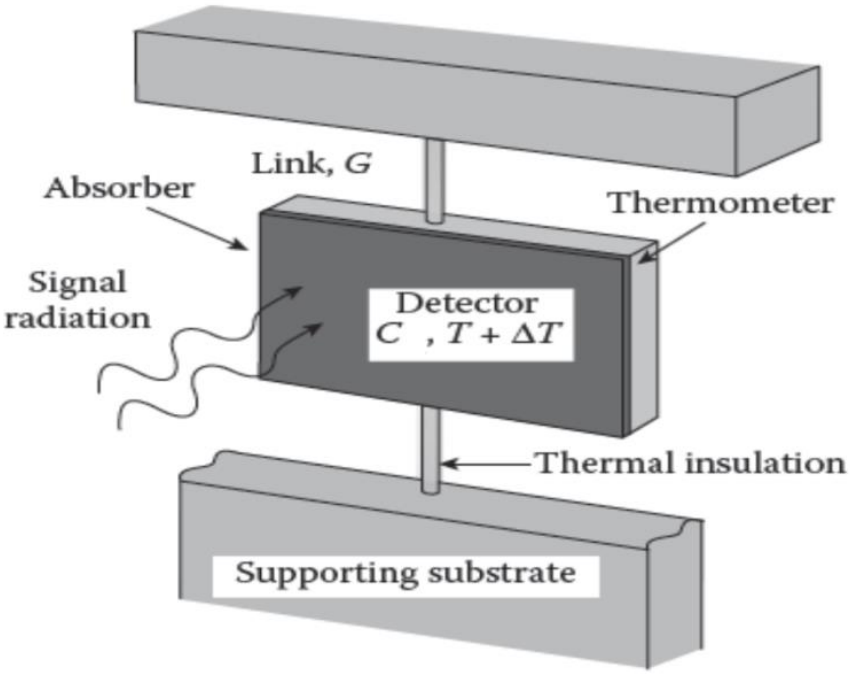

Figure 7. A schematic of a simple thermal detector [46].

The heat capacity C and thermal conductance (G) are given by:

$$C = \text{mass (m)} \times \text{specific heat } (c_p) \quad (1.3)$$

$$G = 4\sigma\varepsilon AT^3 \quad (1.4)$$

where, σ = Stefan-Boltzmann constant

ε = emissivity
A = surface area
T = temperature in Kelvin

The initial temperature of the detector, before the radiation input, is equal to the constant temperature of the sink T_0. However, after the detector absorbs radiation, the temperature of the detector changes by ΔT which is obtained as a solution to the heat balance equation [47, 48],

$$\frac{Cd(\Delta T)}{dt} + G\Delta T = \varepsilon\Phi \quad (1.5)$$

Taking radiant power (Φ) as a periodic function i.e., $\Phi = \Phi_0 e^{i\omega t}$, where Φ_0 is the amplitude of sinusoidal radiation, the solution to equation (1.5) is given by [49],

$$\Delta T = \frac{\varepsilon\Phi_0}{(G^{2+}\omega^2 C^2)^{1/2}} \quad (1.6)$$

Here, time dependent component of the solution involves the exponential term decaying with time and, hence, is ignored. Root mean square (rms) value of the electrical output voltage of the detector, which is proportional to change in temperature, can be written as:

$$\Delta V = K\Delta T = \frac{K\varepsilon\Phi_0}{(G^{2+}\omega^2 C^2)^{1/2}} \quad (1.7)$$

Obviously, a sensing material must be chosen in such a way that we obtain ΔT as large as possible which, in turn, requires, from equation (1.6), that G and C be as small as possible. In other words, while optimizing the interaction between radiation and the detector, the thermal contacts with its surroundings should be minimized. This requires that we choose a small detector mass and fine wire for connecting to the heat sink.

1.3.1. Performance Parameter of a Photodetector

The efficiency of a photodetector is based on several specifications. Normally, the following parameters are used by most manufactures of photodetectors to specify their overall performance.

Responsivity or Sensitivity

Response of a detector is measured in terms of quantities such as current, voltage, wavelength or impulse with respect to incident optical power. For instance, the detector current per unit incident power defines current responsivity (R_I) of the device. In general, responsivity of the detector varies with the wavelength of incident radiation and the responsivity at a particular wavelength is called spectral responsivity. Some other responses such as angular response can also be studied where change in output of the device varies as a function of the angle of incidence.

Quantum Efficiency (η)

Quantum efficiency is the probability that each photon incident on a material produces the charge carrier contributing to the detector current. Since all the incident photons are not absorbed, the quantum efficiency varies within $\mathbf{0} \leq \boldsymbol{\eta} \leq \mathbf{1}$. In practical situation, many photons impinge on the material and quantum efficiency can be taken as the ratio of the flux of charge carriers contributing to the detector current to the flux of incident photons. In the case of surface defects or reflection of radiation, a photon fails to reach the detector and hence only the absorbed photons should be taken into account. In this sense, we can call this parameter an internal quantum efficiency. Mathematically, quantum efficiency is given by [50],

$$\eta = \frac{1.24\, R_I}{\lambda} \times 100\% \tag{1.8}$$

where, λ is the wavelength in μm

α/G ratio

The ratio of absorption coefficient to thermal conductance is the fundamental figure of merit for sensing element and determines the detectivity limits of the photodetector.

Dark Current

The detector current observed even when the photodetector is totally shielded from outside radiation is referred as the dark current.

Linear Dynamic Range

In general, a detector responds linearly with the incident optical power. However, an excessively large optical power degrades responsivity of the device and is said to be saturated. The range over which the detector exhibits linearity is called linear dynamic range.

Optical Gain

When electron-hole pairs are generated by incident photons, charge carriers flow in the detector circuit. Normally, each pair (with two charge carriers) is assumed to produce a charge (q=2e) in the external circuit. However, it has been shown [51] that only a charge of e is produced in the circuit. Moreover, some devices produce charge (q) different from e or 2e. The average number of circuit electrons produced per generated pair is called optical gain and can have the value greater or less than unity.

Noise

Normally all detectors suffer from some sort of noise but the source and degree of noise depend on the choice of materials. Major sources of noise are: shot noise generated by random emission of electrons, radiation noise which includes both signal fluctuation and background fluctuation noise, thermal Johnson noise (or thermal noise or Nyquist noise) generated by random motions of charge carriers at finite temperature, amplifier noise, microphonic noise and Flicker or 1/f noise- the noise which increases rapidly with decrease in frequency and is assumed to originate from material and manufacturing defects.

Noise Equivalent Power (NEP)

Noise equivalent power is defined as the incident optical power required for the detector to produce output signal equal to the noise in the frequency bandwidth of 1 Hz. In other words, NEP is the incident power required to produce signal to noise ratio (S/N) equal to one. Mathematically, NEP is given by,

$$NEP = \frac{I_N}{R_I}, \tag{1.9}$$

where, I_N is the quadrature sum of currents due to all significant noises.

Obviously, it is desired that we obtain a higher value of signal to noise ratio, which requires smaller value of NEP. Hence NEP can be taken as the measure of signal to noise ratio.

Noise Equivalent Temperature Difference (NETD)

Noise equivalent temperature difference (NETD) is the temperature difference between objects in a scene producing a signal-to-noise ratio of 1. The smaller the NETD, higher is the sensitivity and better is the performance of the detector.

Detectivity (D)

This is a figure of merit used for comparing detectors and is defined as inverse of NEP (D=1/NEP).

Specific Detectivity or Area Normalized Detectivity (D*)

This is another figure of merit used to compare detectors of similar spectral response and physical types but with different area.

$$D^* = \frac{(A\,\Delta f)^{1/2}}{NEP} \tag{1.10}$$

where, Δf is the band width of the associated electronics and A is the active area of a detector, the primary light-collecting area of the detector surface, which is different from secondary area in some detectors that absorbs light to generate output signal, called non active area.

Thermal Time Constant or Thermal Response Time

Thermal time constant of a detector shows how quickly a detector responds to the incident IR radiation. It is defined as the ratio of thermal capacity (C) of the sensing element to the thermal conductivity (G). Response time of a detector is typically in the millisecond range for thermal detector which is much longer than for a photon detector. Smaller response time requires small active area of the sensing element but it should be carefully optimized because decrease in area will result in reduction of incident input.

1.3.2. Bolometers

Detection of dangers in advance, superior situation awareness and the use of precise weapon on time (if required) are the main requirements for both military and non military security applications. Infrared detectors, sensitive in both short and long wave infrared region, fulfill most of these requirements [52]. Due to two major performance parameters, excellent signal to noise ratio and fast response time, photon detectors are widely used in IR detector technology. Since the energy of incident photons is comparable to average thermal energies (K_BT) of atoms of the sensing element [53], the noise due to thermal charge carriers is inevitable and hence these photon detectors require cryogenic cooling to 77K or below [54]. Cooling mechanism, included in the photodetectors, make the device not only heavy, bulky and inconvenient but also expensive. Furthermore, photon detectors lack in broad band response i.e., they exhibit selective wavelength dependent response to incident radiation. Lack or difficulty in operating the photon detectors with appropriate spectral response in the IR region [50] is their other drawback. On the other hand, thermal detectors such as thermocouples, bolometers, thermopiles, and pyroelectric detectors are interesting because they are rugged, reliable, light, inexpensive and they can be operated at room temperature. Most of the thermal devices are passive devices for they do not require bias and, most importantly, they provide flatter spectral response. In this section, we will discuss one of the thermal IR detectors - the bolometers (Greek, “bole” meaning- ray). Bolometer was first designed in 1880 by Langley for solar observation; he demonstrated that the device sensitivity increased by 3 orders of magnitude as compared to thermopile and was capable of measuring temperature change as small as 1/100000 of 1^oC [55]. Since then, the bolometer has been widely used in civilian and defense utilities. Figure 8 shows a picture taken from a helicopter using such an IR device in Boston, Massachusetts, during a security operation after the recent Boston marathon bombing on April 15, 2013.

The bolometer consists of a sensing element having strong temperature coefficient of resistance [TCR] so that a small temperature change, caused by incident radiation, can be measured. Unlike semiconductor based photon detectors, resistive bolometers are uncooled, based on simple principle and easy to fabricate. It is possible [57] to fabricate thermal bolometric detectors on thermally isolated hanging membranes by utilizing the recent progress in microelectromechanical systems technology (popularly known as MEMS technology). Due to recent developments in MEMS technology, performance levels of cooled infrared photon detectors have now been maintained by these uncooled infrared bolometers [22]. TCR is one of the vital parameters that influence the performance of bolometer and metals, semiconductors, thermistors and superconducting materials, having sufficient TCR, have been studied as possible candidates for sensing element in the bolometric devices.

Figure 8. Boston marathon bombing suspect found hiding in a boat [56].

The performance of a thermal detector can be divided into two steps: raising the temperature of a sensing material by input radiation and using the temperature dependent variation of a particular property of the material for signaling in the output circuit. The second step, involving the use of material's property, depends on the type of thermal detector and, for bolometer, we use TCR (α) defined by, $\alpha = \frac{1}{R}\frac{dR}{dT}$.. Accordingly, change in voltage of a current biased bolometer becomes,

$$\Delta V = I\Delta R = IR\alpha\Delta T \tag{1.11}$$

Comparing equations (1.7) and (1.11) we get, K=$IR\alpha$ and the equation (1.7) can be rewritten as,

$$\Delta V = \frac{IR\alpha\varepsilon\Phi_0}{(G^{2+}\omega^2C^2)^{1/2}} \tag{1.12}$$

Hence voltage sensitivity of a bolometer is,

$$R_v = \frac{IR\alpha\varepsilon}{(G^{2+}\omega^2C^2)^{1/2}} \tag{1.13}$$

It is seen that the sensitivity is inversely proportional to thermal conductance and thermal capacity. However, the sensitivity is directly influenced by the product of current (I), resistance (R) and TCR (α). Also, high emissivity is desirable in the atmospheric IR window of 8-14 μm bolometric devices.

The simplest representation of a bolometer consists of finding a sensitive material having high α, low thermal mass (C) along with maximum thermal isolation (low G). However, an accurate model of a bolometer requires a complex representation of parameters in the model (some of the important parameters are discussed in section 1.3.1). The performance of bolometers is typically hindered by noises and one of them is 1/f noise, the sources of which are not well understood. The noises vary by several orders of magnitude depending on the sensing material and its composition. 1/f noise has been found to be low for monocrystalline material as compared to amorphous or polycrystalline material. The most common bolometer sensing elements are vanadium oxides (VO_x), silicon diode and amorphous silicon (a-Si). Particularly V_2O_3, which undergoes IMT at low temperature (the critical temperature of transition, T_c=160K), has very low resistance at room temperature and can be used for low noise microbolometers. In addition to V_2O_3, mixed vanadium oxides (VO_x) are becoming popular thermistor materials and are used in the new generation of silicon microbolometers.

Thermistors are known to be stable materials having long life span and resistant to nuclear radiation. Thermistor materials, used in bolometer fabrication, are a mixture of various semiconducting oxides having higher TCR than metals. Their TCR depends on the impurity state, band gap and major conduction mechanism. Since the resistance for a semiconductor varies as $R = R_0 T^{-3/2} \exp\left(\frac{b}{T}\right)$, the TCR at room temperature can be written as $\alpha = -b/T^2$ [46]. This means TCR varies inversely as square of temperature. The TCR of VO_x exceeds 0.03 per ^oC (~2% K^{-1} at 25^oC) which is sufficiently high for use in infrared imaging applications and is, in fact, five to ten times better than the TCR of most metals. VO_x is also found to have favorable optical properties for enhancing IR absorption. VO_x has a measured responsivity of 250,000 V/W in response to 300K blackbody radiation [46]. Because of a good combination of low 1/f noise, high TCR, high electrical resistivity, fabrication capability, good IR absorption characteristics, good passivation characteristics in conjunction with silicon nitride (Si_3N_4), vanadium oxides are suitable candidates as sensing material in bolometers.

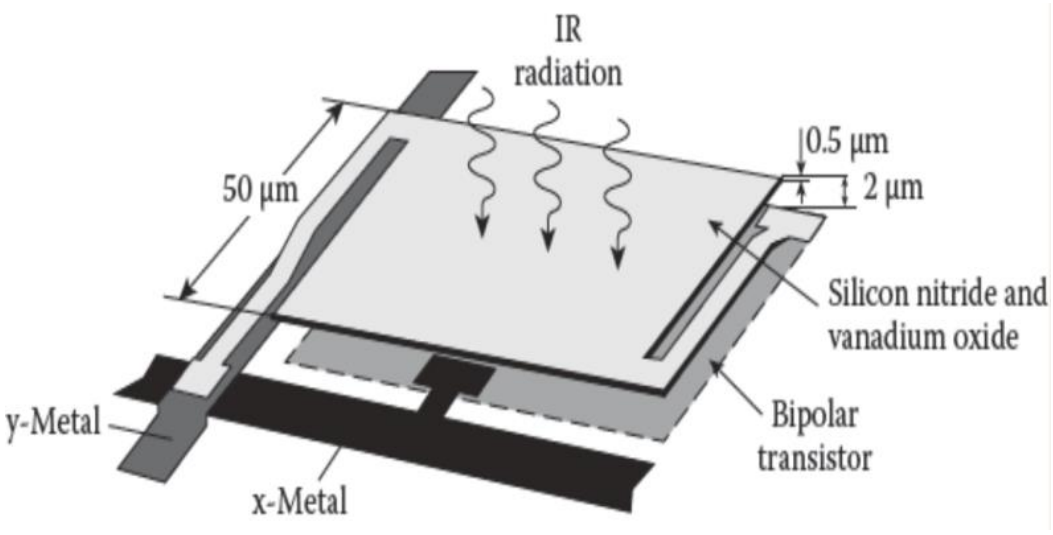

Figure 9. A microbolometer pixel structure [46].

Figure 9 shows the basic design of the Honeywell bolometer, which consists of a two-level structure with a gap of ~ 2 μm between them. The upper level is a square shaped silicon nitride (Si_3N_4) plate, of side 50 μm and thickness 0.5 μm, suspended over an underlying silicon integrated circuit (IC) substrate. A family of fabrication compatible materials with high TCR and well defined resistance can be developed out of mixed oxides of vanadium (VO_2, V_2O_3 and V_2O_5) using low-temperature ion beam sputtering deposition process [24]. Such VO_x films have a resistance of 20KΩ per square film at 25^oC which is quite sufficient for microbolometer readout circuits. The resistor material (VO_x) is, hence, formed within each microstructure plate of Si_3N_4. The bridge structure of Si_3N_4 is also supported by two narrow legs of Si_3N_4 that additionally provide the thermal insulation (since microbolometers require high thermal insulation, we do not rely on air insulation but on the microstructure support). The legs also contain a thin metal layer and hence serve as an electrical contact. A bipolar transistor is normally required for amplification purposes. An aluminum layer on the substrate reflects the absorbed IR radiation back to the sensing material and thus maximizes the absorption process. A monolithic control circuit is fabricated in the silicon substrate so that individual leadouts from each microstructure of a large number of individual microstructure arrays can be avoided. The basic purpose of the monolithic circuit is to apply a control voltage to each microstructure in the array and hence measure the microstructure resistance.

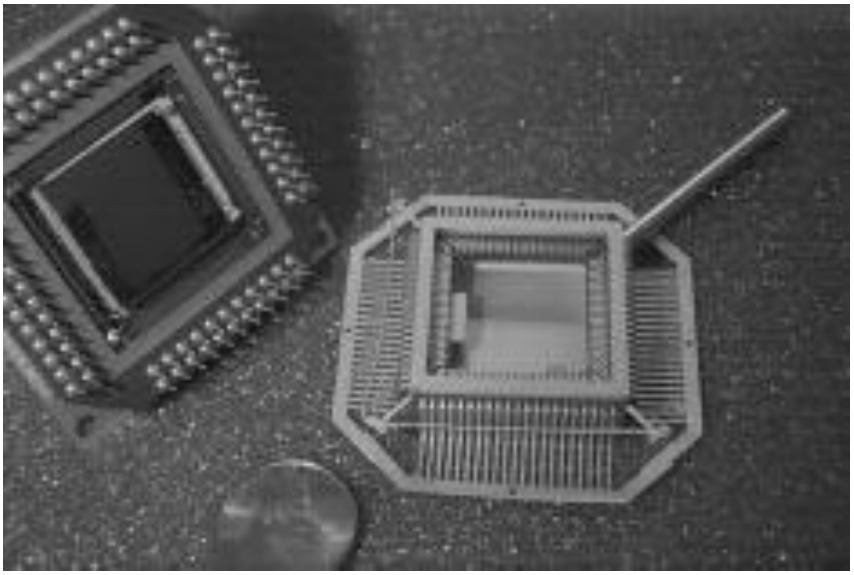

Figure 10. A ceramic package of microbolometer arrays operating at room temperature [24].

A prototype of an uncooled IR camera, operating at room temperature, was constructed out of such 240×336 microbolometer arrays as shown in Figure 10. This is a small micromachined structure extremely well thermally isolated from the substrate ($G=10^{-7}$ W/K) and having very small thermal mass ($C=10^{-9}$ J/K and corresponds to a thermal time constant of 10 ms). This thermal isolation is close to the maximum possible physical limit of about 10^{-8} W/K for a 50 μm square detector. With a microbolometer resistance of 50KΩ and TCR of 2%/K, it was shown [24] that a typical IR signal of 1 nW was enough to change the microbolometer

temperature by 0.01 K. This resulted in the value of the thermal signal to noise ratio as 275. Furthermore, Honeywell has claimed that the microbridge of Si_3N_4 is such a strong structure that it can tolerate shocks of several thousand g-forces (weight per unit mass). Tables 1 and 2 show the list of performance parameters for the VO_x bolometer.

Table 1. Performance parameters for a typical VO_x bolometer

Parameter	TCR (K^{-1})	Responsivity (V/W)	Resistance (KΩ/square	G (W/K)	C (J/K)	T (ms)	S/N
Value	~2% @298K	250,000 @300K	20 @ 298K	$G=10^{-7}$	10^{-9}	10	>275

Table 2. Performance parameter, NETD, for commercial VO_x bolometers (mK @ f-number of infrared optics =1 and frequency= 20-60 Hz) [58]

Company	FLIR USA	L-3 USA	BAE USA	Raytheon USA	DRS USA	NEC Japan	SCD Israel
NETD	35	50	30-50	30-50	35-50	75	50

The monolithic silicon bolometer technology was developed, for the first time in early 1980s, in Honeywell Sensor and System Development Center in Minneapolis, Minnesota. Later, both Honeywell (on VO_x) and Texas Instruments (on a-Si) worked under classified projects sponsored by DARPA and U.S. Army Night Vision and Electronic Sensor Directorate and finally succeeded in producing low-cost night vision systems with NEDT of 0.1^oC using f/1 optics. Today, thermistor bolometers are widely used in applications such as fire detection systems, radiometer, space-borne horizon sensors, burglar alarms and industrial temperature measurements. They are also useful in applications requiring flat spectral response. In 2005, John Fluke Mfg. Co. had introduced a number of models of hand-held, portable infrared cameras of commercial standard. A stable, high TCR bolometer material of mixed vanadium oxides was the key to the success of the room temperature, uncooled bolometer at Honeywell.

1.4. METAMATERIALS

The term metamaterials (Greek, "meta" meaning- beyond) was coined by Walser [59] in 1999. Literally speaking, metamaterials are artificially designed materials which have properties that may not exist in nature. According to Munk [60], Walser defined metamaterials as "macroscopic composites having man-made, three-dimensional, periodic cellular architecture designed to produce an optimized combination, not available in nature, of two or more responses to specific excitation". Among the scientific community, metamaterials, today, are popularly recognized as composite materials which simultaneously possess negative permeability (μ) and permittivity (ε) (In order to be consistent with the standard notation, we have chosen ε to symbolize permittivity and readers should not be confused with emissivity of section 1.3). Even when both the constitutive parameters of a material are negative, $\varepsilon\mu$ is positive and hence wave propagation is still possible. However,

for the sake of energy conservation, we must choose negative sign in $n = \pm\sqrt{\varepsilon\mu}$ [61, 62]. Accordingly, such a medium can be characterized by negative refractive index and said to form a "left handed" medium in which Cherenkov radiation, Doppler effect and even Snell's laws are reversed [63]. Depending on the sign of ε and μ, materials can be classified as shown in Figure 11.

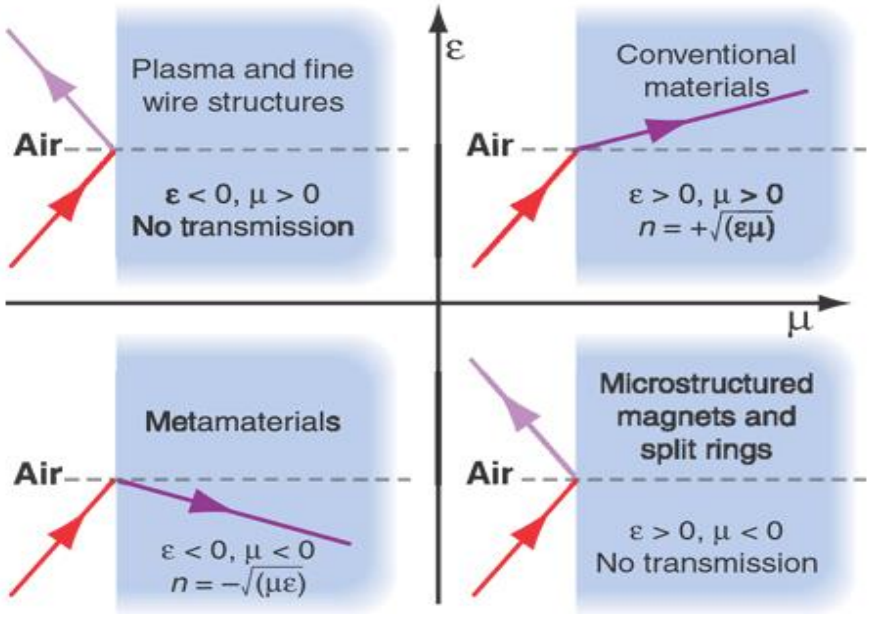

Figure 11. Classification of materials according to μ and ε [62].

Figure 12. A microwave invisible cloak - might be useful for evading radar [64]. It is worthwhile to note here that radar detects the microwave sent from its antenna, after it is reflected back from a remote target.

Normally, the electromagnetic properties of metamaterials are defined by the way they are structured, not by their chemical composition. The graded structure of an inhomogeneous material such as metal-dielectric composites and metamaterials, where materials properties change gradually as a function of position, can provide stronger nonlinear optical response as

compared to its homogeneous counterpart [65]. Gradation can either be achieved naturally or be engineered in the manufacturing process. Graded materials can be useful for controlling the physical properties of optical materials. It is the gradations of refractive index of metamaterials that lead to its invisibility. This technology can be used to cause an object, from an individual to spaceship, either partially or totally invisible to parts of the electromagnetic spectrum. A plane coated with a metamaterial can elude detection since metamaterials can result in zero reflectance for all incident angles. Hence, they have enormous applications in the defense and security sectors. Figure 12 shows a cloaking device which is practically invisible when viewing the world in microwaves of a particular wavelength. Similarly, we might have a flat superlens operating in the visible spectrum and then we will have images even smaller than one wavelength of light with ultrahigh resolution [66]. Metamaterials have drawn the attention of the scientific community due to their wide range of potential applications.

RESONANCE TUNING USING VANADIUM OXIDES: A RECENT PROGRESS

The capacity of a metamaterial to interact with radiation of certain frequencies in a strong and a special manner is known as its so called resonant behavior. Scientists have been able to device metamaterials working at a single frequency [67] or narrow band [68] in the microwave or infrared regions of the spectrum, terahertz domain [69] and even in the lower end of the visible spectrum [70]. Recently, research in metamaterials is progressing by overcoming the limitations of bandwidth and the dynamic control of metamaterial's properties in real time has been achieved either through non linear responses or externally tunable components. Particularly, after Pendry et al. [71] introduced the concept of split ring resonator (SRR), scientists have constructed metamaterials using SRR [63] and further research has been conducted towards the creation of tunable metamaterials using SSR. It is the dynamically controllable metamaterial that allows us to take advantage of the full potential of its peculiar properties. Shadrivov et al. [72] "took the first step towards the creation and study of fully controlled, tunable nonlinear metamaterial systems through the study of the tunability and self-induced nonlinear response of a single SRR." In his study, Shadrivov used a specially doped p-n junction diode: the variation of diode capacitance led to the change in resonance conditions of the SRR in microwave region. Significant progress has been made towards the study of tunable metamaterials [26, 28, 73-98] and has been core research in modern science and technology.

Particularly, Driscoll et al. [26] have achieved dynamic tuning, with a tuning range of at least 20%, in the near infrared region by using a device made of a 100nm thick gold SRR array and 90nm thick VO_2 film grown on sapphire substrate. Both the gold and VO_2 layers are much thinner than the periodicity of SRR array (20μm) and are said to form an effective (single) material layer. This structure is now considered as a hybrid metamaterial since it has the combined property of both SRR and VO_2. It is well established that VO_2 undergoes insulator metal phase transition (IMT), on a sub-picosecond timescale [99], as a result of some external stimuli. At the onset of the phase transition, nanoscale (5 -10nm) metallic grains or "puddles" emerge from the insulating host of VO_2. The percolative nature of the

phase transition causes divergent permittivity. This drastic change in optical behavior has a strong effect on the resonance frequency of the SRR metamaterial - the local electromagnetic fields of the SRR gets modified as if a tunable dielectric were inside a capacitor. It is found that the resonance frequency of the hybrid system varies inversely with the change in permittivity of VO_2. Furthermore, the decrease in metallic puddles damps the resonance amplitude.

Wen *et al.*[100] have proposed VO_2 cut-wire fabricated on silica-glass substrate as a terahertz metamaterial. The advantage of cut-wire resonator over SRR is that it exhibits simple yet broad band response [101-105]. Furthermore, cut-wire resonators are easy to design and fabricate. Motivated by the 4 orders of magnitude change observed in the dielectric properties of VO_2 during IMT, researchers are rigorously busy to find out whether the same order of magnitude change in extinction can be obtained in metamaterials [106]. Furthermore, due to the pronounced hysteresis present in phase transition [20], scientist are interested in designing memory metamaterials where the metamaterial tuning persists even if triggering stimulus for IMT disappears [25]. A wide variety of structures based on VO_2 phase transition have been studied in recent years due to the versatile properties of VO_2 [28, 106-111]. More interestingly, some researchers have identified VO_2 as a natural disordered metamaterial [112].

REFERENCES

[1] G. Kotliar, D. Vollhardt, Physics Today 57 (2004) 53-59.
[2] C. Lamsal, N. M. Ravindra, J. Mat. Sci. 48 (2013) 6341-6351.
[3] A. Zylbersztejn, N. F. Mott, Phys. Rev. B 11 (1975) 4383-4395.
[4] F. Morin, Phys. Rev. Lett. 3 (1959) 34-36.
[5] G. S. Nadkarni, V. S. Shirodkar, Thin Solid Films 105 (1983) 115-129.
[6] D. M. Lamb. Semiconductor to Metalic Phase Transitions from Vanadium and Titanium Oxides Induced by Visible Light. Missouri State University (2009).
[7] C. Batista, R. M. Ribeiro, V. Teixeira, Nanoscale Res. Lett. 6 (2011) 301 (7 pages).
[8] A. Cavalleri, C. Tóth, C. W. Siders, J. A. Squier, F. Ráksi, P. Forget, J. C. Kieffer, Phys. Rev. Lett. 87 (2001) 237401 (4 pages).
[9] C. Wessel, C. Reimann, A. Müller, D. Weber, M. Lerch, T. Ressler, T. Bredow, R. Dronskowski, J. Comput. Chem. 33 (2012) 2102-2107.
[10] E. E. Chain, Appl. Opt. 30 (1991) 2782-2787.
[11] P. D. Dernier, M. Marezio, Phys. Rev. B 2 (1970) 3771-3776.
[12] F. Chudnovskiy, S. Luryi, B. Spivak, Switching device based on first-order metalinsulator transition induced by external electric field, in: S. Luryi, J. M. Xu, A. Zaslavsky, (Eds.) Future Trends in Microelectronics: the Nano Millennium, Wiley Interscience (2002) pp. 148-155.
[13] C. G. Granqvist, Phys. Scripta 32 (1985) 401-407.
[14] V. S. -Milosevic, N. Nilius, H. -P. Rust, H. -J. Freund, Phys. Rev. B 77 (2008) 125112.
[15] J. B. K. Kana, J. M. Ndjaka, P. O. Ateba, B.D. Ngom, N. Manyala, O. Nemraoui, A. C. Beye, M. Maaza, Appl. Surf. Sci. 254 (2008) 3959-3963.

[16] M.S. Thomas, J.F. DeNatale, P. J. Hood, Materials Research Society Symposium Proceedings 479 (1997) 161-166.
[17] Z. Zhang, Y. Gao, H. Luo, L. Kang, Z. Chen, J. Du, M. Kanehira, Y. Zhang, Z. L. Wang, Energy & Environ. Sci. 4 (2011) 4290-4297.
[18] C. G. Granqvist, Handbook of Inorganic Electrochromic Materials. Elsevier Science, Amsterdam, Holland (1995).
[19] A. Gupta, R. Aggarwal, P. Gupta, T. Dutta, R. J. Narayan, J. Narayan, Appl. Phys. Lett. 95 (2009) 111915 (3 pages).
[20] T. Driscoll, H. -T. Kim, B. -G. Chae, M. D. Ventra, D. N. Basov, Appl. Phys. Lett. 95 (2009) 043503 (3 pages).
[21] L.A.L. D. Almeida, G.S. Deep, A.M.N. Lima H. Neff, Appl. Phys. Lett. 77 (2000) 4365 (3 pages).
[22] F. Niklaus, A. Decharat, C. Jansson, G. Stemme, Infrared Physics & Technology, 51 (2008) 168-177.
[23] R.T.R. Kumar, B. Karunagaran, D. Mangalaraj, S. K. Narayandass, P. Manoravi, M. Joseph, V. Gopal, Sens Actuat. A: Physical, 107 (2003) 62-67.
[24] B.E. Cole, R. E. Higashi, R. A. Wood, Proceedings of the IEEE, 86 (1998) 1679-1686.
[25] T. Driscoll, H.-T. Kim, B. -G. Chae, B. -J. Kim, Y. -W. Lee, N. M. Jokerst, S. Palit, D. R. Smith, M. D. Ventra, D. N. Basov, Science 325 (2009) 1518-1521.
[26] T. Driscoll, S. Palit, M.M. Qazilbash, M. Brehm, F. Keilmann, B. -G. Chae, S. -J. Yun, H.-T. Kim, S. Y. Cho, N. M. Jokerst, D. R. Smith, D. N. Basov, Appl. Phys. Lett. 93 (2008) 024101 (3 pages).
[27] M.J. Dicken, K. Aydin, I. M. Pryce, L. A. Sweatlock, E. M. Boyd, S. Walavalkar, J. Ma, H. A. Atwater, Opt. Exp. 17 (2009) 18330-18339.
[28] J.S. Kyoung, M. A. Seo, S. M. Koo, H. R. Park, H. S. Kim, B. J. Kim, H. T. Kim, N. K. Park, D. S. Kim, K. J. Ahn, Phys. Status Solidi C 8 (2011) 1227-1230.
[29] A. Ritter, Smart Materials in Architecture, Interior Architecture and Design. Basel, Switzerland: Birkhäuser (2007).
[30] C.M. Lampert, Materials Today, 7 (2004) 28-35.
[31] J. Bell, M. Schwartz, Smart Materials. Boca Raton, Florida: CRC Press (2009).
[32] http://en.wikipedia.org/wiki/Smart_glass (Date: 06/27/2013: 1:10 pm).
[33] S.K. Deb, Appl. Opt. Supp. 1 (1969) 192-195.
[34] C.G. Granqvist, E. Avendaño, A. Azens, Thin Solid Films, 442 (2003) 201-211.
[35] P. R. Somani, S. Radhakrishnan, Mat. Chem. Phys. 77 (2002) 117-133.
[36] M.S.R. Khan, K.A. Khan, W. Estrada, C. G. Granqvist, J. Appl. Phys. 69 (1991) 3231-3234.
[37] S. F. Cogan, N. M. Nguyen, S. J. Perrotti, R. D. Rauh, J. Appl. Phys. 66 (1989) 1333-1337.
[38] A. Talledo, A. M. Andersson, C. G. Granqvist, J. Mat. Res. 5 (1990) 1253-1256.
[39] A. M. Andersson, C. G. Granqvist, J. R. Stevens, Appl. Opt. 28 (1989) 3295-3302.
[40] A. Talledo, C.G. Granqvist, J. Appl. Phys. 77 (1995) 4655-4666.
[41] D.W. ullett, J. Phys. C: Solid State Physics, 13 (1980) L595-L599.
[42] M.A. Sobhan, R. T. Kivaisi, B. Stjerna, C. G. Granqvist, Solar Energy Mat. Solar Cells, 44 (1996) 451-455.
[43] C.G. Granqvist, Thin Solid Films, 193-194 (1990) 730-741.
[44] C. G. Granqvist, Solar Energy Mat. Adv. Mat. 15 (2003) 1789-1803.

[45] J. Art, Photon Detectors for Confocal Microscopy, in: Pawley, J.B. (Ed.) Handbook of Biological Confocal Microscopy, Springer Science + Business Media, LLC, New York, 2006.
[46] A. Rogalski, Infrared detectors. Boca Raton: CRC Press (2011).
[47] A. Rogalski, Infrared detectors. Amsterdam: Gordon and Breach (2000).
[48] E.L. Dereniak, G.D. Boreman, Infrared Detectors and Systems. New York: Wiley (1996).
[49] A. Rogalski, A., Quantum Well Infrared Photoconductors in Infrared Detectors Technology, in: Ryzhii, V. (Ed.) Intersubband Infrared Photodetectors, World Scientific New Jersey, pp. 1-66 (2003).
[50] S.C. Stotlar, Infrared detector, in: Waynant, R. & Ediger, M. (Eds.) Electro-Optics Handbook McGraw-Hill, New York, 200, pp. 17.11-17.24.
[51] B.E.A. Saleh, M. C. Teich, Fundamentals of Photonics. New Jersey: Wiley-Interscience (2007).
[52] R. Breiter, M. Münzber, IR modules and devices for security applications, in: Beyerer, J. (Ed.) Future Security: 2nd Security Research Conference, Germany, pp. 96-99 (2007).
[53] G. Hyseni, N. Caka, K. Hyseni, Infrared Thermal Detectors Parameters: Semiconductor Bolometers Versus Pyroelectrics. Wseas Transactions on Circuits and Systems, 9, 238-247 (2010).
[54] R.B. Darling, S. Iwanaga, Sadhana, 34 (2009) 531-542.
[55] S. P. Langley, The Bolometer. Nature 25 (1881), 14-16.
[56] http://photoblog.nbcnews.com/_news/2013/04/20/17841024-infrared-police-chopper-images-show-boston-marathon-suspect-hiding-in-boat?lite (Date: 07/28/2013: 3:05 pm).
[57] R. K. Bhan, R. S. Saxena, C. R. Jalwania, S. K. Lomash, Defence Science Journal, 59 (2009) 580-589.
[58] F. Niklaus, C. Vieider, H. Jakobsen, MEMS-based uncooled infrared bolometer arrays: a review. Proc. SPIE, 6836 (2008) 68360D (15 pages).
[59] R. Walser, Metamaterials: An Introduction, in: Weiglhofer, W.S. & Lakhtakia, A. (Eds.) Introduction to Complex Mediums for Optics and Electromagnetics, SPIE-The International Society for Optical Engineering, Bellingham, Washington, pp. 295-316 (2003).
[60] B.A. Munk, Metamaterials : critique and alternatives. Hoboken, New Jersey: John Wiley & Sons, Inc. (2009).
[61] J.B. Pendry, hys. Rev. Lett. 85 (2000) 3966-3969.
[62] M.C.K. Wiltshire, Science 292 (2001) 60-61.
[63] D.R. Smith, W. J. Padilla, D. C. Vier, S. C. N. -Nasser, S. Schultz, Phys. Rev. Lett. 84 (2000) 4184-4187.
[64] A. Cho, Science 314 (2006) 403.
[65] J.-P. Huang, K. W. Yu, New Nonlinear Optical Materials: Theoretical Research. New York: Nova Science Publishers, Inc. (2013)
[66] C. M. Soukoulis, Optics & Photonics News, 17, 16-21 (2006).
[67] D. Schurig, J. J. Mock, B.J., Justice, S. A. Cummer, J. B. Pendry, A. F. Starr, D. R. Smith, Science 314 (2006) 977-980.

[68] T. Driscoll, D. N. Basov, A. F. Starr, P. M. Rye, S. N. -Nasser, D. Schurig, D. R. Smith, Appl. Phys. Lett. 88 (2006) 081101 (3 pages).
[69] S. Linden, C. Enkrich, M. Wegener, J. Zhou, T. Koschny, C. M. Soukoulis, Science 306 (2004) 1351-1353.
[70] C.M. Soukoulis, S. Linden, M. Wegener, Science 315 (2007) 47-49.
[71] J. B. Pendry, A. J. Holden, D. J. Robbins, W. J. Stewart, IEEE Transactions on Microwave Theory and Techniques 47 (1999) 2075-2084.
[72] I.V. Shadrivov, S.K. Morrison, Y.S. Kivshar, Opt. Exp. 14 (2006) 9344-9349.
[73] P.V. Kapitanova, S.I. Maslovski, I.V. Shadrivov, P.M. Voroshilov, D.S. Filonov, P.A. Belov, Y.S. Kivshar, Appl. Phys. Lett. 99 (2011) 251914 (3 pages).
[74] I.V. Shadrivov, A.B. Kozyrev, D.W.V.D. Weide, Y. S. Kivshar, Opt. Exp. 16 (2008) 20266-20271.
[75] I.V. Shadrivov, A.B. Kozyrev, D.W.V.D. Weide, Y. S. Kivshar, Appl. Phys. Lett. 93 (2008) 161903 (3 pages).
[76] Y. Wang, J. Yin, G. Yuan, X. Dong, C. Du, Appl. Phys. A, 104 (2011) 1243-1247.
[77] D. Shrekenhamer, S. Rout, A. C. Strikwerda, C. Bingham, R. D. Averitt, S. Sonkusale, W. J. Padilla, Opt. Exp. 19 (2011) 9968-9975.
[78] Z. Wang, Y. Luo, L. Peng, J. Huangfu, T. Jiang, D. Wang, H. Chen, L. Ran, Appl. Phys. Lett. 94 (2009) 134102 (3 pages).
[79] H.-T. Chen, J. F. O'Hara, A. K. Azad, A. J. Taylor, R. D. Averitt, D. B. Shrekenhamer, W. J. Padilla, Nature Photonics 2 (2008) 295 - 298.
[80] D. Mittleman, Nature Photonics 2 (2008) 267 - 268.
[81] Q. Zhao, L. Kang, B. Du, B. Li, J. Zhou, H. Tang, X. Liang, B. Zhang, Appl. Phys. Lett. 90 (2007) 011112 (3 pages).
[82] D.H. Werner, D.-H. Kwon, I.-C. Khoo, A.V. Kildishev V. M. Shalaev, Opt. Exp. 15 (2007) 3342-3347.
[83] R. Pratibha, K. Park, I.I. Smalyukh, W. Park, Opt. Exp. 17 (2009) 19459-19469
[84] Y. Poo, R.-X. Wu, G.-H. He, P. Chen, J. Xu, R. -F. Chen, Appl. Phys. Lett. 96 (2010) 161902 (3 pages).
[85] G. He, R. -X. Wu, Y. Poo, P. Chen, J. Appl. Phys. 107 (2010) 093522 (5 pages).
[86] J. Han, A. Lakhtakia, C. -W. Qiu, Opt. Exp. 16 (2008) 14390-14396.
[87] M. Lapine, D. Powell, M. Gorkunov, I. Shadrivov, R. Marqués, Y. Kivshar, Appl. Phys. Lett. 95 (2009) 084105 (3 pages).
[88] M. Lapine, I. V. Shadrivov, D. A. Powell, Y. S. Kivshar, Nature Materials 11 (2012) 30-33.
[89] W.M. Zhu, A. Q. Liu, X. M. Zhang, D. P. Tsai, T. Bourouina, J. H. Teng, X. H. Zhang, H. C. Guo, H. Tanoto, T. Mei, G. Q. Lo, D. L. Kwong, Adv. Mat. 23 (2011) 1792-1796.
[90] Y.H. Fu, A. Q. Liu, W. M. Zhu, X. M. Zhang, D.P. Tsai, J. B. Zhang, T. Mei, J. F. Tao, H. C. Guo, X. H. Zhang, J. H. Teng, N. I. Zheludev, G. Q. Lo, D. L. Kwong, Adv. Func. Mat. 21 (2011) 3589-3594.
[91] D.A. Powell, K. Hannam, I.V. Shadrivov, Y.S. Kivshar, *Phys. Rev. B* 83 (2011) 235420 (6 pages).
[92] H. Liu, Y. M. Liu, T. Li, S. M. Wang, S.N. Zhu, X. Zhang, *Phys. Status Solidi* (b) 246 (2009) 1397-1406.

[93] F. Hesmer, E. Tatartschuk, O. Zhuromskyy, A. A. Radkovskaya, M. Shamonin, T. Hao, C. J. Stevens, G. Faulkner, D. J. Edwards, E. Shamonina, Phys. Status Solidi (b) 244 (2007) 1170-1175.
[94] J.Y. Ou, E. Plum, L. Jiang, N. I. Zheludev, Nano Letters 11 (2011) 2142-2144.
[95] H. Tao, A. C. Strikwerda, K. Fan, W. J. Padilla, X. Zhang, R. D. Averitt, Phys. Rev. Lett. 103 (2009) 147401 (4 pages).
[96] X.G. Peralta, M.C. Wanke, C.L. Arrington, J.D. Williams, I. Brener, A. Strikwerda, R. D. Averitt, W. J. Padilla, E. Smirnova, A. J. Taylor, J. F. O'Hara, Appl. Phys. Lett. 94 (2009) 161113 (3 pages).
[97] H. Tao, A. C. Strikwerda, K. Fan, C. M. Bingham, W. J. Padilla, X. Zhang, R. D. Averitt, J. Phys. D: Appl. Phys. 41 (2008) 232004 (5 pages).
[98] I.E. Khodasevych, C.M. Shah, S. Sriram, M. Bhaskaran, W. Withayachumnankul, B.S.Y. Ung, H. Lin, W.S.T. Rowe, D. Abbott, A. Mitchell, Appl. Phys. Lett. 100 (2012) (3 pages).
[99] A. Cavalleri, T. Dekorsy, H.H.W. Chong, J. C. Kieffer, R. W. Schoenlein, Phys. Rev. B 70 (2004) 161102(R) (4 pages).
[100] Q.-Y. Wen, H.-W. Zhang, Q.-H. Yang, Y.-S. Xie, K. Chen, Y.-L. Liu, Appl. Phys. Lett. 97 (2010) 021111 (3 pages).
[101] L.V. Panina, A. N. Grigorenko, D. P. Makhnovskiy, Phys. Rev. B 66 (2002) 155411 (17 pages).
[102] A. N. Lagarkov, A. K. Sarychev, Phys. Rev. B 53 (1996) 6318-6336.
[103] V.A. Podolskiy, A.K. Sarychev, E.E. Narimanov, V.M. Shalaev, J. Opt. A: Pure and Appl. Opt. 7 (2005) S32-S37.
[104] L. Fu, H. Schweizer, H. Guo, N. Liu, H. Giessen, Phys. Rev. B 78 (2008) 115110 (9 pages).
[105] G. Dolling, C. Enkrich, M. Wegener, J. F. Zhou, C. M. Soukoulis, S. Linden, Opt. Lett. 30 (2005) 3198-3200.
[106] M. Seo, J. Kyoung, H. Park, S. Koo, H.-S. Kim, H. Bernien, B. J. Kim, J. H. Choe, Y. H. Ahn, H. -T. Kim, N. Park, Q. -H. Park, K. Ahn, D.- S. Kim, Nano Lett. 10 (2010) 2064-2068.
[107] M. Liu, H. Y. Hwang, H. Tao, A. C. Strikwerda, K. Fan, G. R. Keiser, A. J. Sternbach, K. G. West, S. Kittiwatanakul, J. Lu, S. A. Wolf, F. G. Omenetto, X. Zhang, K. A. Nelson, R. D. Averitt, Nature 487 (2012) 345.
[108] T. Paik, S. -H. Hong, T. Gordon, A. Gaulding, C. Kagan, C. Murray, (2013) http://meetings.aps.org/link/BAPS.2013.MAR.C19.13.
[109] Q.-Y. Wen, H.-W. Zhang, Q.-H. Yang, Z. Chen, Y. Long, Y.-L. Jing, Y. Lin, P. -X. Zhang, J. Phys. D: Appl. Phys. 45 (2012) 235106-235110.
[110] W.-X. Huang, X.-G. Yin, C.-P. Huang, Q.-J. Wang, T.-F. Miao, Y.-Y. Zhu, Appl. Phys. Lett. 96 (2010) 261908 (3 pages).
[111] K. Appavoo, F. Richard, J. Haglund, Nano Letters 11 (2011) 1025-1031.
[112] M.A. Kats, R. Blanchard, S. Zhang, P. Genevet, C. Ko, S. Ramanathan, F. Capasso, Vanadium dioxide as a natural disordered metamaterial: perfect thermal emission and large broadband negative differential thermal emittance. arXiv:1305.0033 [physics.optics] (2013).